Dynamic models for LES of turbulent front propagation with a spectral method

By H. G. Im[1], T. S. Lund, AND J. H. Ferziger

1. Motivation and objectives

Direct numerical simulation of turbulent reacting flows places extreme demands on computational resources. At the present time, simulations can be performed only for greatly simplified reaction systems and for very low Reynolds numbers. Direct simulation of more realistic cases occurring at higher Reynolds number and including multiple species and numerous chemical reactions will exceed available computational resources far into the future. Because of this, there is a clear need to develop the technique of large eddy simulation for reacting flows. Unfortunately this task is complicated by the fact that combustion arises from chemical reactions that occur at the smallest scales of the flow. Capturing the large-scale behavior without resolving the small-scale details is extremely difficult in combustion problems. Thus LES modeling for turbulent combustion encounters difficulties not present in modeling momentum transport, in which the main effect of the small scales is to provide dissipation. The difficulty is more pronounced in premixed combustion, where detailed chemistry plays an essential role in determining the flame speed (or overall burning rate); in nonpremixed combustion infinite rate chemistry can be assumed, eliminating the small scale features to a first approximation.

One of the practically relevant and better understood types of turbulent premixed combustion is the laminar flamelet regime, in which the characteristic chemical time is much shorter than the characteristic flow time (Liñán & Williams 1993). Under this condition, combustion can be represented in terms of the propagation of laminar flamelets corrugated by turbulent eddies. It has been suggested (Kerstein *et al.* 1988) that such a propagating front may be captured by defining the front as a level contour of a continuous function G, whose governing equation is

$$\frac{\partial G}{\partial t} + u_j \frac{\partial G}{\partial x_j} = S_L |\nabla G|. \tag{1}$$

In this equation, all information about the flame structure is carried by the flame speed S_L. This provides a convenient opening for large eddy simulation; the flame structure need not be modeled. Since the flame retains its laminar structure, explicit expressions for S_L as a function of the flow variables may be taken from asymptotic studies (e.g., Clavin 1985) or computations.

In LES, only *filtered* flame fronts are resolved. These fronts can be viewed as flame brushes that propagate at a speed, $\bar{S}$, higher than the laminar flame speed.

[1] Present address: Sandia National Laboratories

The problem is closed if one can provide an explicit expression for $\bar{S}$ as a function of available quantities. Several previous studies have attempted to derive relationships between $\bar{S}$ and the turbulence intensity u' (Clavin & Williams 1979, Yakhot 1988a, Kerstein and Ashurst 1992, Pocheau 1992). However, the existing theoretical and empirical results for $\bar{S}(u')$ do not agree with one another, so the functional form of $\bar{S}(u')$ remains an open question. Even if the question is resolved, there will be a constant or function to be determined.

In this study, we present an attempt at LES using a dynamic subgrid-scale model that has been successfully applied to a variety of turbulent flows (Germano *et al.* 1991). The basic formulation was derived earlier (Im 1995), but the model is modified to incorporate the effect of subgrid transport. In contrast to previous LES approaches for the G-equation (Menon *et al.* 1993), the model constants are computed dynamically as a part of the calculation procedure rather than being prescribed. Dynamic modeling for turbulent flow has been shown to exhibit correct behavior, for example, in the near-wall region of boundary layers, without the need for additional modification. The LES models for the G-equation suggested in this study have these features, allowing the possibility of application to practical combustion systems.

2. Accomplishments

2.1 Some remarks on the G-equation

Before we proceed with LES modeling, some numerical issues related to the G-equation should be pointed out. If one wishes to solve Eq. (1) in the Huygens' limit, i.e. $S_L = S_L^\circ$, numerical difficulties arise due to the formation of cusps as the front propagates. Cusps are a natural consequence of the Huygens' process in much the same way as shocks are a characteristic feature of Burger's equation. To overcome the numerical difficulty associated with cusps, previous studies introduced various types of diffusive terms (e.g. Kerstein *et al.* 1988). These terms are not entirely *ad hoc*, however; they can be shown to represent the effect of thermal relaxation under transverse heat diffusion in the preheat zone of a wrinkled front (Clavin 1985). Using the asymptotic relation for S_L, Eq. (1) can be written as

$$\frac{\partial G}{\partial t} + u_j \frac{\partial G}{\partial x_j} = S_L^\circ |\nabla G| + \mathcal{D}\nabla^2 G, \tag{2}$$

where only the leading term has been kept; this is a reasonable approximation provided the flame thickness is sufficiently smaller than the hydrodynamic scale. In the above relation, $\mathcal{D} = S_L^\circ \mathcal{L}$ is the Markstein diffusivity, where the Markstein *length*, $\mathcal{L}$, is typically normalized by the flame thickness ℓ_F. Since

$$\ell_F = \alpha / S_L^\circ = (1/S_L^\circ)(\nu/Pr),$$

we find

$$\mathcal{D} = (\nu/Pr)Ma$$

where ν is the molecular viscosity, Pr the Prandtl number, and $Ma = \mathcal{L}/\ell_F$ the Markstein number, which is $O(1)$ in practical flames (Searby & Quinard 1990).

We attempt to solve Eq. (2) with a given value of $\mathcal{D}$; the results depend on this parameter. Numerical realization of the Huygens' limit (i.e. $\mathcal{D} \to 0$) is extremely difficult, if not impossible. Our numerical simulations of the passive G-equation in isotropic turbulence revealed that the overall flame speed depends significantly on the size of the diffusion term in the G-equation. This is not surprising; it demonstrates that one must be careful about choosing this term, especially when comparing the flame speed with experiments. Accurate estimation of the Markstein number is mandatory for such comparisons.

Due to the lack of experimental results, in this study LES models are validated by comparing with DNS results based on Eq. (2) with 64^3 resolution. Most of the LES are performed in 32^3 resolution using the filtered DNS fields as initial conditions.

2.2 Subgrid-scale models for the G-equation

We now describe the dynamic subgrid-scale models for the passive G-equation. As in turbulence, we assume scale invariance of the G-equation in the inertial range of turbulence, which has been shown to exist by Yakhot (1988b) and Pocheau (1992). We define the grid filter $\bar{\mathcal{G}}$ and the test filter $\hat{\mathcal{G}}$ respectively as

$$\bar{f}(\mathbf{x}) = \int f(\mathbf{x}')\bar{\mathcal{G}}(\mathbf{x},\mathbf{x}')d\mathbf{x}', \qquad \hat{f}(\mathbf{x}) = \int f(\mathbf{x}')\hat{\mathcal{G}}(\mathbf{x},\mathbf{x}')d\mathbf{x}',$$

where the width of the test filter, $\hat{\Delta}$, is larger than that of the grid filter, Δ. Applying the grid filter to Eq. (2), we obtain

$$\frac{\partial \bar{G}}{\partial t} + \frac{\partial}{\partial x_j}\left(\bar{u}_j \bar{G}\right) = -\frac{\partial}{\partial x_j}\left(\overline{u_j G} - \bar{u}\bar{G}\right) + S_L^\circ \overline{|\nabla G|} + \mathcal{D}\frac{\partial^2 \bar{G}}{\partial x_j^2}. \tag{3}$$

Here both the subgrid scalar flux $\overline{u_j G} - \bar{u}_j \bar{G}$ and the filtered modulus term $\overline{|\nabla G|}$ need to be modeled. In the previous study (Im 1995), these two terms were modeled by a single *filtered* propagation term, $\bar{S}|\nabla \bar{G}|$. This model, however, suffered from numerical instability since no subgrid dissipation was provided. In this study, the subgrid flux term is modeled by an eddy diffusivity model analogous to the Smagorinsky model, *i.e.*:

$$\gamma_k = \overline{u_k G} - \bar{u}_k \bar{G} = -\alpha_t \frac{\partial \bar{G}}{\partial x_k}, \qquad \alpha_t = C_G \Delta^2 |\bar{\Sigma}|, \tag{4}$$

where $|\bar{\Sigma}|$ is the magnitude of the strain rate tensor:

$$|\bar{\Sigma}| = (2\bar{\Sigma}_{ij}\bar{\Sigma}_{ij})^{1/2}, \quad \bar{\Sigma}_{ij} = \frac{1}{2}\left(\frac{\partial \bar{u}_i}{\partial x_j} + \frac{\partial \bar{u}_j}{\partial x_i}\right). \tag{5}$$

Similarly, at the test filter level, we obtain

$$\Gamma_k = \widehat{\overline{u_k G}} - \hat{\bar{u}}_k \hat{\bar{G}} = -\hat{\alpha}_t \frac{\partial \hat{\bar{G}}}{\partial x_k}, \qquad \hat{\alpha}_t = C_G \hat{\Delta}^2 |\hat{\bar{\Sigma}}|. \tag{6}$$

and a generalization of Germano's identity

$$\mathcal{F}_k = \Gamma_k - \hat{\gamma}_k = \widehat{\bar{u}_k \bar{G}} - \hat{\bar{u}}_k \hat{\bar{G}} \tag{7}$$

can be used to determine the constant C_G. Using Eqs. (4), (6), and (7) with the least-square contraction (Lilly 1992), we obtain

$$C_G \Delta^2 = -\frac{\mathcal{F}_i \mathcal{H}_i}{\mathcal{H}_j \mathcal{H}_j}, \tag{8}$$

where

$$\mathcal{H}_k = (\hat{\Delta}/\Delta)^2 |\hat{\bar{\Sigma}}| \frac{\partial \hat{\bar{G}}}{\partial x_k} - \widehat{|\bar{\Sigma}| \frac{\partial \bar{G}}{\partial x_k}}. \tag{9}$$

Next we consider the modeling of the propagation term, $S_L^\circ \overline{|\nabla G|}$. This requires a special treatment as it contains a nonlinear modulus. We adopt the following model

$$S_L^\circ \overline{|\nabla G|} = \bar{S} |\nabla \bar{G}|. \tag{10}$$

The effective flame speed, $\bar{S}$, can be related to the laminar flame speed by requiring that the filtered equations maintain the correct overall burning rate. This constraint gives rise to the notion of representing the "filtered propagation term" as "propagation of the filtered front at higher speed", and may be characterized by writing

$$S_L^\circ A_L = \bar{S} \bar{A}, \tag{11}$$

where A_L is the laminar flame area that would be computed in a direct simulation, and $\bar{A}$ is the area of the filtered flame front. For incompressible isotropic turbulence, the flame area can be readily computed as (Kerstein *et al.* 1988)

$$A_L = \langle |\nabla G| \rangle, \quad \bar{A} = \langle |\nabla \bar{G}| \rangle, \tag{12}$$

where the bracket denotes the volume average. Furthermore, it is necessary to determine $\bar{S}$ as a function of turbulence intensity. Theoretical studies suggest the functional form

$$\bar{S}/S_L^\circ = 1 + C_S (q/S_L^\circ)^p \tag{13}$$

where $q = [\overline{(u_i - \bar{u}_i)(u_i - \bar{u}_i)}]^{1/2}$ is the square-root of the subgrid kinetic energy in the filter volume. Previous studies (Clavin & Williams 1979, Pocheau 1992) show that quadratic ($p = 2$) and linear ($p = 1$) behaviors are expected in the weak and strong turbulence limits, respectively. In the next section, this functional relation will be examined using an *a priori* test based on DNS data.

Given the value of p, the constant C_S can be determined by a dynamic procedure. Combining (11), (12), (13) and applying the same model to the test-filtered quantities, we obtain

$$\frac{\bar{S}}{S_L^\circ} = \frac{A_L}{\bar{A}} = \frac{\langle |\nabla G| \rangle}{\langle |\nabla \bar{G}| \rangle} = \left\langle 1 + C_S \left(\frac{q}{S_L^\circ} \right)^p \right\rangle, \tag{14}$$

$$\frac{\hat{\bar{S}}}{S_L^\circ} = \frac{A_L}{\hat{\bar{A}}} = \frac{\langle|\nabla G|\rangle}{\langle|\nabla\hat{\bar{G}}|\rangle} = \left\langle 1 + C_S\left(\frac{Q}{S_L^\circ}\right)^p\right\rangle, \tag{15}$$

where $Q = [(u_i - \hat{\bar{u}}_i)(u_i - \hat{\bar{u}}_i)]^{1/2}$ is the square-root of the subgrid kinetic energy associated with the test filter. It is readily seen that there are two unknowns, $\langle|\nabla G|\rangle$ and C_S, and two equations, provided the subgrid kinetic energies, q and Q, are available. This requires an additional model for the subgrid kinetic energy as a function of the large-scale quantities. As will be seen later, unlike the case of Smagorinsky's model, the model for the subgrid kinetic energy is crucial to accurate prediction of the flame speed. We shall consider the following three models:

1. $q \sim \Delta|\bar{\Sigma}|$, deduced from dimensional reasoning similar to that used in Smagorinsky's model. Since $\bar{\Sigma}$ can be computed, this model is applicable with any numerical method. Unfortunately, this model overpredicts the turbulent flame speed when the turbulence is not in the inertial subrange, as will be shown later.

2. Spectral curve fit, which can be used with spectral methods. The turbulence energy spectrum is described by an algebraic power relation

$$E(k) = C_k k^{-m}, \tag{16}$$

or an exponential

$$E(k) = C_k \exp(-mk). \tag{17}$$

The two unknowns C_k and m can be determined from $E(\bar{k})$ and $E(\hat{k})$. The subgrid kinetic energy can then be computed as

$$q(\bar{k}) = \int_{\bar{k}}^{\infty} E(k)dk. \tag{18}$$

3. Since the spectral curve fit has limited application, we suggest another model similar to that of Bardina *et al.* (1983). We define a new filter with size $\tilde{\Delta}$, where $\Delta < \tilde{\Delta} < \hat{\Delta}$. Then the subgrid kinetic energies are estimated by

$$q^2 = \bar{u}_i\bar{u}_i - \tilde{\bar{u}}_i\tilde{\bar{u}}_i, \tag{19}$$

and

$$Q^2 = \hat{\bar{u}}_i\hat{\bar{u}}_i - \check{\bar{u}}_i\check{\bar{u}}_i, \tag{20}$$

where $\tilde{\Delta}/\Delta = \check{\Delta}/\hat{\Delta} = 1.4 \approx \sqrt{2}$ are used in the present calculation.

In the following section, *a priori* tests are performed by applying these models (referred to as Models 1, 2, and 3) for the propagation term, combined with the Smagorinsky-type subgrid transport model.

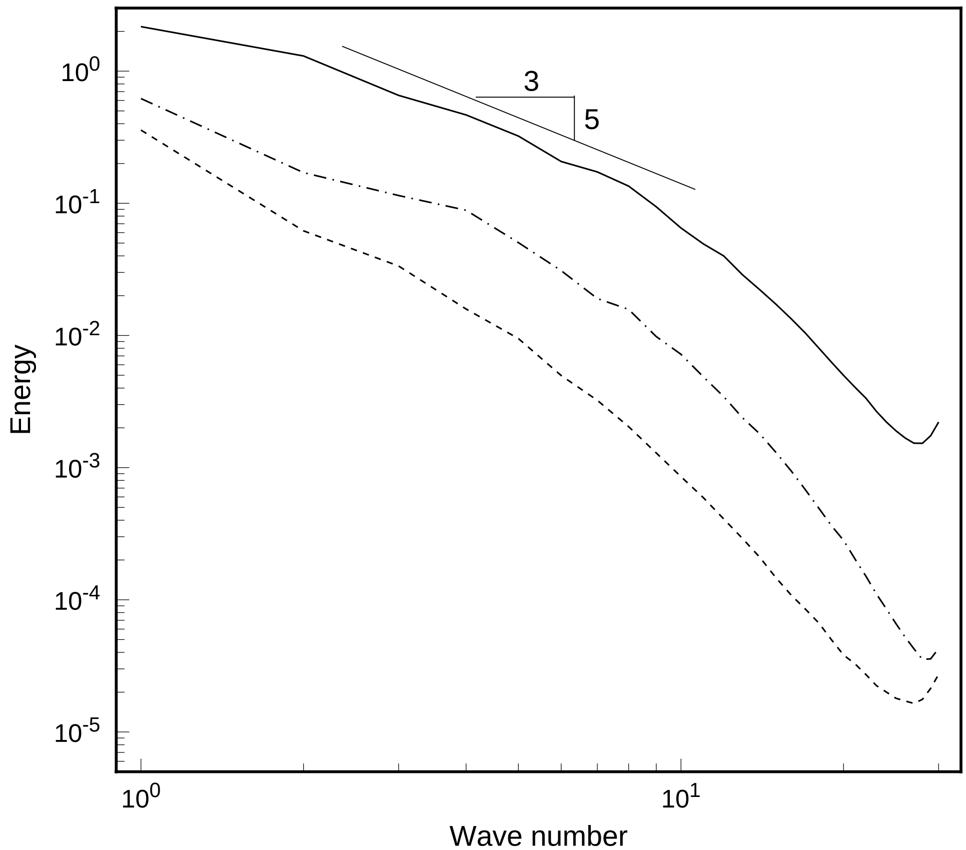

FIGURE 1. Energy spectra obtained from the DNS, 3.6 large-eddy turnover times after the g-field was initialized. Turbulence energy: ——— ; scalar energy $(g'^2/2)$ for $u'/S_L^\circ = 0.5$: - - - - ; energy in g fluctuations for $u'/S_L^\circ = 2$: —·— .

2.3 A priori tests of the models

The subgrid models proposed in §2.2 are tested by post-processing DNS results. We performed DNS based on Eq. (2) with incompressible homogeneous isotropic turbulence. The turbulence is forced at the lowest wavenumbers in order to hold the total kinetic energy approximately constant. The numerical method is pseudo-spectral is space with second order Runge-Kutta time integration (Rogallo 1981). A developed flow field is used as the initial condition and the G-field is initialized as a linear function $G = x$. To make the G-field homogeneous, we define $g = G - x$ and solve for g. Following initialization of the g field, the simulation is run for 3.6 large-scale eddy turn over times, at which point the g field is fully-developed. The Reynolds number based on Taylor microscale is about 75 and $Ma/Pr = 4$, so $\mathcal{D} = 4\nu$. Two cases were computed; $u'/S_L^\circ = 0.5$ and 2, which was accomplished by adjusting S_L° for the same turbulence field.

Figure 1 shows the DNS results for the turbulence and scalar energy (g'^2) spectra for both values of u'/S_L°. The slope $-5/3$ is also shown. It is seen that the turbulence spectrum has a slope $-5/3$ over a limited range of k due to the low Reynolds number

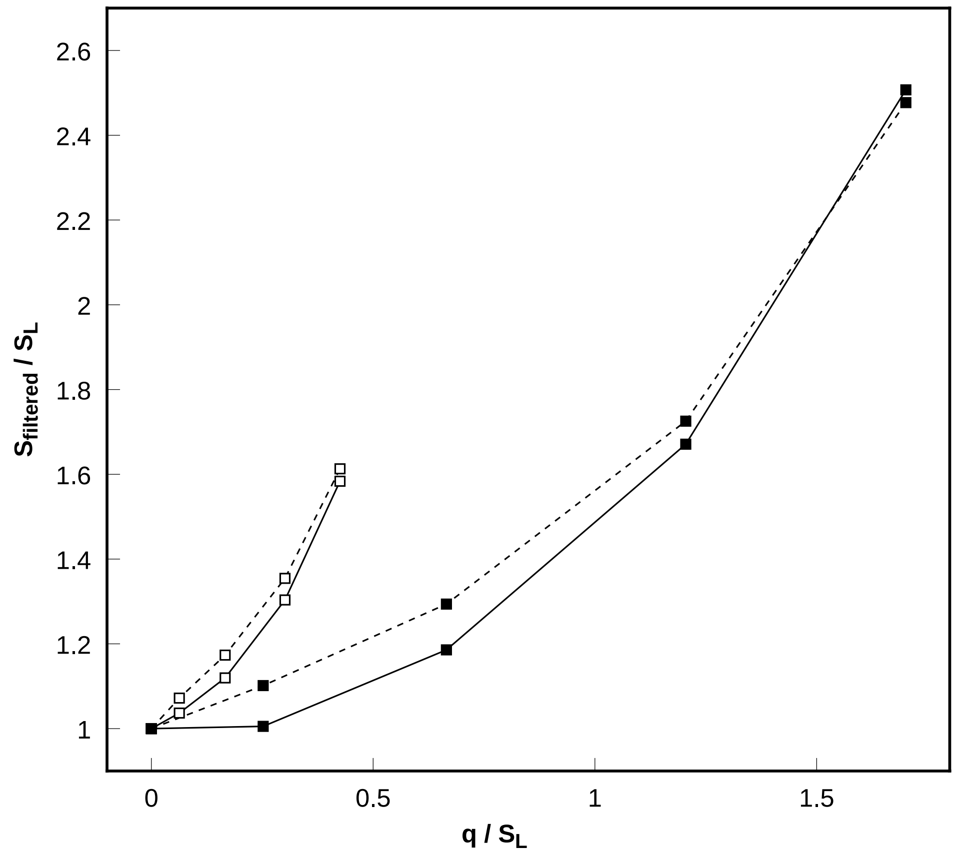

FIGURE 2. Enhanced filtered flame speed $\bar{S}/S_L^\circ$ vs. normalized subgrid kinetic energy q/S_L°. Cutoff filter: ——— ; Gaussian filter: ---- ; $u'/S_L^\circ = 0.5$: □ ; $u'/S_L^\circ = 2$: ■ .

of the flow.

Since the Smagorinsky-type transport model has been established in previous LES studies, the main emphasis in this work is on the modeling of the propagation term. We first examine the functional relation of $\bar{S}/S_L^\circ$ and q/S_L°. These quantities are computed from the DNS spectrum by using

$$q = \int_{\bar{k}}^{\infty} 2E(k)dk, \tag{20}$$

$$\bar{S}/S_L^\circ = \langle |\nabla G| \rangle / \langle |\nabla \bar{G}| \rangle. \tag{21}$$

To obtain the filtered field $\bar{G}$, we use (a) the cutoff filter in the Fourier space, and (b) the Gaussian filter $\mathcal{G}(k) = \exp(-k^2\Delta/24)$. Although the cutoff filter is more relevant with the spectral method, the Gaussian filter is more practical with finite difference techniques.

Figure 2 shows $\bar{S}/S_L^\circ$ as a function of q/S_L° for various filter sizes; increased abscissa corresponds to increased filter size. It is seen that while the Gaussian filter

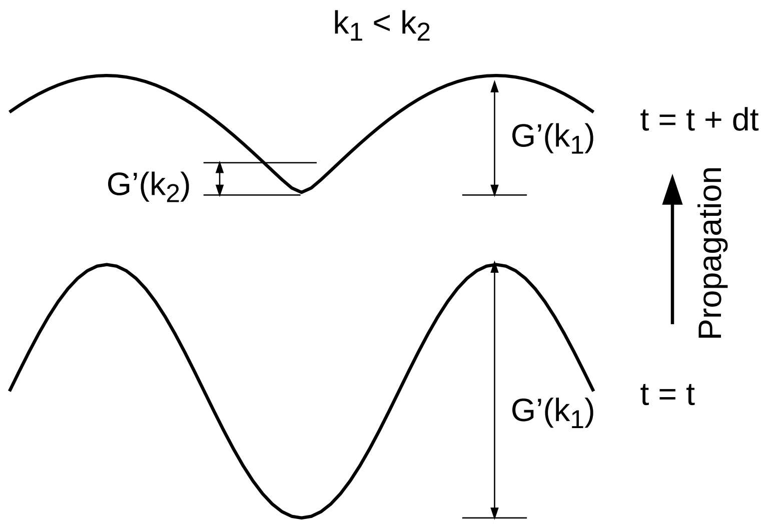

FIGURE 3. Schematic showing the mechanism of kinematic restoration by the flame propagation.

gives approximately linear behavior at very small q/S_L°, with the cutoff filter the increase in $\bar{S}/S_L^\circ$ is much less significant and the curves exhibit quadratic behavior from the start. This observation is in contrast to an earlier result that showed linear behavior (Bourlioux *et al.* 1996). Incidentally, the quadratic behavior is consistent with a theoretical prediction of Clavin & Williams (1979) for weak turbulence.

It is noted that the nonlinear behavior shown in Fig. 2 is more prominent in the stronger turbulence case, $u'/S_L^\circ = 2$. The reason can be found from Fig. 1; for stronger turbulence ($u'/S_L^\circ = 2$) the fluctuations in the G-function are controlled more by the turbulence than by the propagation and there is more scalar energy at low wavenumbers. Physically, as shown schematically in Fig. 3, propagation diminishes front corrugation, which is called "kinematic restoration" by Peters (1992), while small-scale wrinkles are formed at the trough, which will lead to cusp formation in the Huygens' limit. Therefore, one effect of propagation is to transfer energy from low to high wave-numbers. Consequently, the higher u'/S_L°, i.e. the less significant the propagation, the more the nonlinearity in Fig. 2, because less energy is present at high wavenumbers. Since the cutoff filter is used in the present spectral calculation, we choose $p = 2$ for most of our calculations.

Next we use the DNS data to check the accuracy of the model for the effective propagation defined in section 2.2. To do this, the 64^3 DNS field is used to compute the actual flame speed, taken as the volume average of $|\nabla G|$. Then the DNS field is filtered to 32^3 by truncating the high wavenumbers. This cutoff-filtered field is then used to compute the filtered flame speed, which is the target for the model.

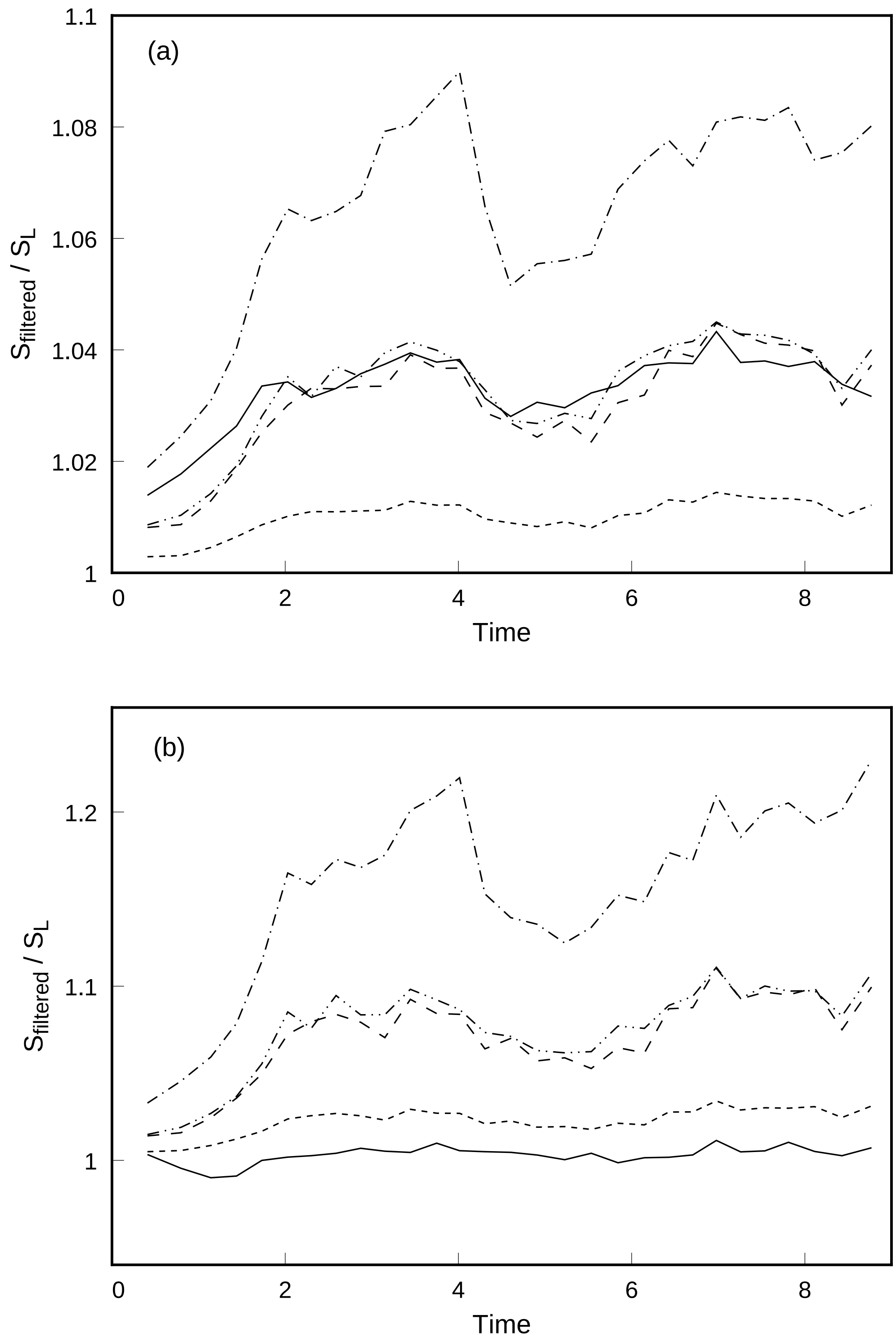

FIGURE 4. *A priori* tests of the filtered flame speed $\bar{S}$ for various models; (a) $u'/S_L^\circ = 0.5$, (b) $u'/S_L^\circ = 2$. Direct DNS result: ——— ; Model 1: —·— ; Model 2 with the power law: — — — ; Model 2 with the exponential law: - - - - ; Model 3: —··— .

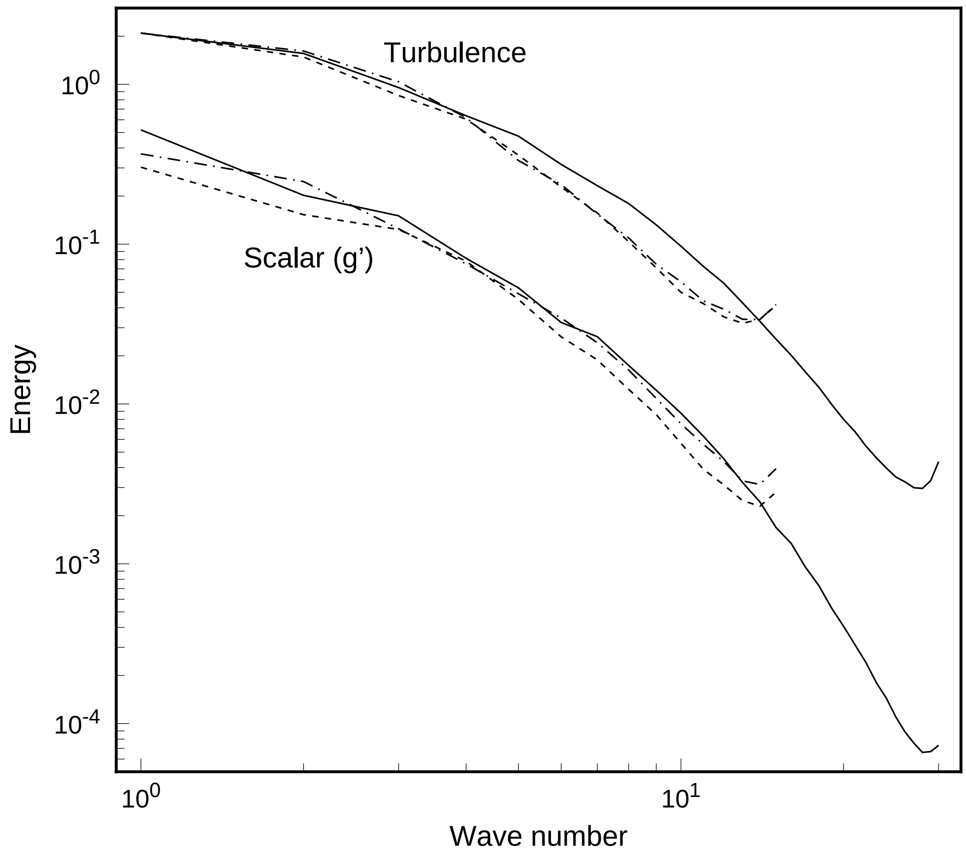

FIGURE 5. Comparison of energy spectra obtained from DNS and various LES models for $u'/S_L^\circ = 2$ at 3.6 eddy turnover time after the g-field was initialized; DNS: ——— ; LES with Model 1: —·— ; LES with Model 2 with the exponential law: ---- .

Using only the filtered information, Eqs. (14) and (15) are solved for $\bar{S}/S_L$, for each of the three models for the subgrid kinetic energy. In order to test the validity of Eq. (15), a second "test filtering" of the DNS data is made by truncating to 16^3 modes. Finally the procedure is repeated at each time step in the DNS from the initialization of the g field to the end of the run, 3.6 large-scale turnover times later.

Figures 4(a) and (b) show $\bar{S}/S_L^\circ$ computed from various subgrid kinetic energy models at various times during the DNS, for $u'/S_L^\circ = 0.5$ and 2, respectively. A quadratic functional relation ($p = 2$) was assumed. In both cases, it is clear that Model 1 overpredicts the filtered flame speed. This may be due to the low Reynolds number of this flow. For $u'/S_L^\circ = 0.5$, both model 2 with the power law and model 3 give good results. On the other hand, for $u'/S_L^\circ = 2$, for which less energy is contained in the subgrid scales, the actual $\bar{S}/S_L^\circ$ is much smaller than that predicted by Model 2 with the power law and Model 3, but Model 2 with the exponential law gives better agreement. These results indicate that the prediction of turbulent flame speed using LES of the G-equation depends strongly on accurate estimation of subgrid turbulent kinetic energy.

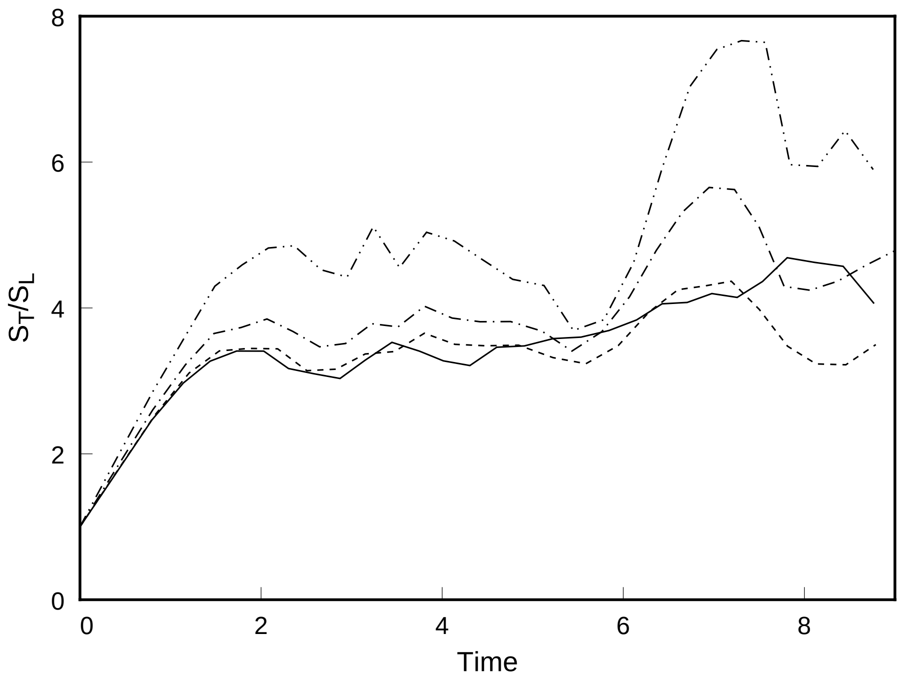

FIGURE 6. Volume averaged turbulent flame speed as a function of time, for $u'/S_L^\circ = 2$; DNS: ——— ; LES with Model 1, $p = 1$: —··— ; LES with Model 1, $p = 2$: —·— ; LES with Model 2, exponential law and $p = 2$: - - - - . Time is scaled by 0.4 large-scale eddy turnover times.

2.4 Results of LES runs

We now present results of actual LES using the suggested dynamic models; this is sometimes called *a posteriori* testing. The initial flow field of the DNS is truncated to 32^3 resolution and used as the initial field for $\bar{u}$, and $\bar{G} = x$ initially.

Figure 5 shows the turbulence and scalar energy spectra of DNS and various LES results at a time 3 large-scale eddy turnover times after initialization of the g field. Two subgrid kinetic energy models are tested: Model 1 (a poor model) and the exponential fit version of Model 2 (the best model). The LES energy spectrum is in fair agreement with the DNS, although it appears that the subgrid-scale model is slightly over-dissipative. The scalar energies of both LES cases agree fairly well with the DNS, while the energy of Model 1 is higher than the exponential spectral fit model, as might be expected from Fig. 4.

Finally, the volume-averaged turbulent flame speed, represented by $\bar{S}\langle|\nabla\bar{G}|\rangle$, is plotted as a function of time in Fig. 6. Results from the DNS are plotted as the solid line. To illustrate the effects of the improvements in the model, results for Model 1 with $p = 1$ are also shown. This simple model may overpredict the turbulent front speed by as much as a factor of two; significant improvement is obtained by merely switching to the quadratic relation ($p = 2$). Model 2 with the exponential curve fit gives the best result in this case since the scalar spectrum falls more rapidly with wavenumber for stronger turbulence.

3. Conclusions and future work

Dynamic models for LES of the G-equation of turbulent premixed combustion have been proposed and tested. Several such models were tested in forced homogeneous isotropic turbulence. The results indicate that, unlike the case for Smagorinsky's model applied to the momentum equation, the estimate of the subgrid kinetic energy is crucial to accurate prediction of turbulent flame speed. For the cases studied here, the extended Smagorinsky model overpredicts the flame speed. Furthermore, $\bar{S}/S_L^\circ$ is not necessarily a linear function of q/S_L°; quadratic dependence seems to fit the results more accurately.

From the differences between the cases with $u'/S_L^\circ = .5$ and 2, it appears that the inability to fit $\bar{S}/S_L^\circ$ as a function of q/S_L° with a fixed value of p is mainly due to the non-similarity between the turbulence and scalar energy spectra in Fig. 1. A modification is proposed to improve the model; one can free the exponent p and use the dynamic procedure to determine it. This requires two levels of test-filters and complicates the numerical procedure.

Finally, we remark that although in the present work G is treated as a passive scalar, the concept can be extended to include heat release. The challenge is a numerical issue of how to capture discontinuities across highly corrugated flames while resolving the small-scale turbulence. Methods designed to resolve this issue have been proposed (Klein 1995, Bourlioux *et al.* 1996), but further work is still needed.

Acknowledgments

The authors would like to thank Prof. A. Bourlioux at CERCA, Université de Montréal for the stimulating discussions during the CTR Summer Program in 1996, and Drs. G. R. Ruetsch and N. S. A. Smith for helpful comments.

REFERENCES

Bardina, J., Ferziger, J. H. & Reynolds, W. C. 1983 Improved subgrid-scale models based on large eddy simulation of homogeneous, incompressible, turbulent flows. *Report TF-19* Dept. Mech. Eng., Stanford University, Stanford, CA.

Bourlioux, A., Klein, R. & Moser, V. 1996 A dynamic subgrid scale model for turbulent premixed flames. *Technical report, CERCA, Montreal.*

Bourlioux, A., Im, H. G. and Ferziger, J. H. 1996 A dynamic subgrid-scale model for LES of the G-equation, *Proceedings of the 1996 Summer Program.* Center for Turbulence Research, NASA Ames/Stanford Univ., 137-148.

Clavin, P. 1985 Dynamic behavior of premixed flame fronts in laminar and turbulent flows. *Prog. Energy Combust. Sci.* **11,** 1.

Clavin, P. & Williams, F. A. 1979 Theory of premixed-flame propagation in large-scale turbulence. *J. Fluid Mech.* **90,** 589.

GERMANO, M., PIOMELLI, U., MOIN, P. & CABOT, W. H. 1991 A dynamic subgrid-scale eddy viscosity model. *Phys. Fluids A.* **3,** 1760.

IM, H. G. 1995 Study of turbulent premixed flame propagation using a laminar flamelet model. *Annual Research Briefs*, Center for Turbulence Research, NASA Ames/Stanford Univ., 347-358.

KERSTEIN, A. R. & ASHURST, WM. T. 1992 Propagation rate of growing interfaces in stirred fluids. *Phys. Rev. Lett.* **68,** 934.

KERSTEIN, A. R., ASHURST, WM. T., & WILLIAMS, F. A. 1988 Field equation for interface propagation in an unsteady homogeneous flow Field. *Phys. Rev. A.* **37,** 2728.

KLEIN, R. 1995 The level set approach to premixed turbulent combustion in the flamelet regime: theory and numerical implementation. *Lecture Notes, Euroconference on Premixed Combustion, Aachen.*

LILLY, D. K. 1992 A proposed modification of the Germano subgrid-scale closure method. *Phys. Fluids A.* **4,** 633.

LIÑÁN, A. & WILLIAMS, F. A. 1993 *Fundamental Aspects of Combustion*, Oxford University Press.

MENON, S. AND KERSTEIN, A. R. 1992 Stochastic simulation of the structure and propagation rate of turbulent premixed flames. *24th Symp. (Int'l) on Combustion*, The Combustion Institute, 443-450.

PETERS, N. 1992 A spectral closure for premixed turbulent combustion in the flamelet regime. *J. Fluid Mech.* **242,** 611.

POCHEAU, A. 1992 Front propagation in a turbulent medium. *Europhysics Letters.* **20,** 401.

ROGALLO, R. 1981 Numerical experiments in homogeneous turbulence, *NASA Tech. Memo.*, TM81315.

SEARBY, G. & QUINARD, J. 1990 Direct and indirect measurements of Markstein numbers of premixed flames. *Comb. Flame.* **82,** 298.

YAKHOT, V. 1988a Propagation velocity of premixed turbulent flames. *Comb. Sci. Tech.* **60,** 191.

YAKHOT, V. 1988b Scale invariant solutions of the theory of thin turbulent flame propagation. *Comb. Sci. Tech.* **62,** 127.